Study of CMS Pixel Sensors

Rafael Aoude[1] and Daniel Pitzl[2]

[1]PUC-Rio - Pontifical Catholic University of Rio de Janeiro
[2]DESY

September 4, 2013

Abstract

The new pixel sensor for the CMS Upgrade requires test and also simulation. This summer student project intend to test some psi46digV2 chips and simulate them. For test, the DESY Testbeam 21, with 4.4 GeV e^+ was used and for the simulation, pixelav and Geant4

Contents

1 Introduction

The CMS (Compact Muon Solenoid) is one of the general purpose experiment in the Large Hadron Collider at CERN. The LHC is a proton-proton collider, with $\sqrt{s} = 7 - 14TeV$ center of mass energy and luminosity of $\mathcal{L} = 10^{34}cm^{-2}s^{-1}$. The proton bunches collides at a rate of 40 MHz and the aim of CMS is to have a good particle track reconstruction, get the momentum and energy information and a good particle identification. To allow this CMS has several types of detectors: Silicon Tracker Detector (Pixel and Strip), Eletromagnetic and Hadronic Calorimeter and Muon Chambers. The Silicon Tracker Detector consists in three layers of pixel detector and ten of strips. Momentum of particles are one of the most important information for a collison, so a good track reconstruction is crucial, for that the pixel sensor are very important. CMS is preparing for an upgrade aimming to put one more layer of pixel silicon to get a better resolution, and also change the readout from analog to digital. Those prototypes with digital readout are being tested at DESY at the DESY TestBeam. This report describes two simulation for the TestBeam and the analysis of the TestBeam Data.

1.1 CMS

In the Figure 1 it shown a slice of the CMS and the tracks of: Muon, Electron, Pion and Photon

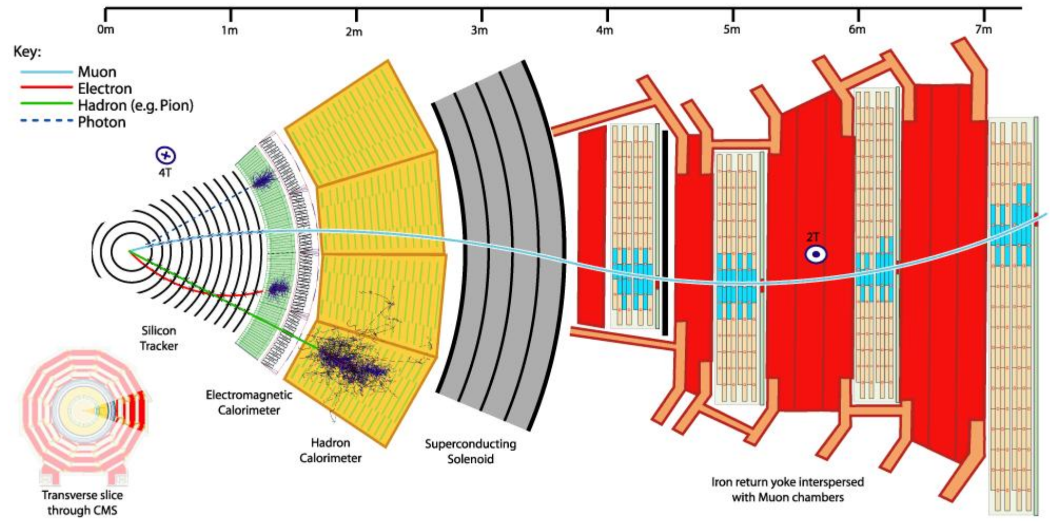

Figure 1: CMS Slice

1.2 CMS Pixel Detector

The CMS pixel detector is the inner detector of CMS. The aim of this detector is precise track reconstruction, for that it is required: High granularity, radiation hardness, small radiation length and good spatial resolution. It has a barrel shape and consists in three layes of barrel and four end disks, that can be described by the subsequent Table 1 and 2 [7]:

Table 1: Parameteres of CMS Pixel Barrel

	Radius [mm]	Faces	full/half Modules	Chips	Pixels	Area $[m^2]$
Layer 1	41-45	18	128/32	2304	6.35×10^6	0.15
Layer 2	70-74	30	224/32	3840	10.6×10^6	0.25
Layer 3	107-112	46	352/32	5888	16.2×10^6	0.38

Table 2: Parameteres of CMS pixel end disk

z	Radius [mm]	Blades	Sensor	Chips Modules	Pixels	Area $[m^2]$
± 32.5	60-150	24	7	1080	3.0×10^6	0.07
± 46.5	60-150	24	7	1080	3.0×10^6	0.07

1.3 Sensor

The sensor constains 4160 pixels of $100\mu m \times 150\mu m$ and $285\mu m$ thick organized in 52 columns and 80 rows. But the sensor is grouped with double columns, that share the buffer at the periphery of the chip.The CMS adopted $n-on-n$ technology, shown in Figure 1.3 it means high dose n-type implant (n^+) pixel at a n-type substrate bulk. The pn junction is done at the back of the sensor with a high-dose p-type implant. Also the pixel are surronded by a guard-ring to prevent voltage breakdown. The $n-on-n$ technology means that when a particle passes through the sensor, it ionize and creates electron-holes pairs, the eletrons are collected by the pixel creating a signal for the ReadOut Chip (ROC).

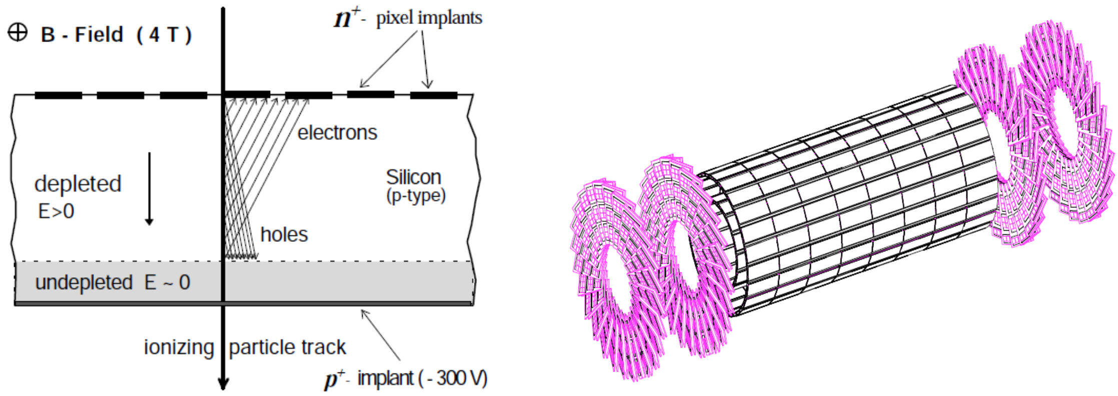

(a) Pixel Sensor (b) Barrel and End Disk Layout

1.4 ROC

Each sensor is connected via bump bond to its own readout circuit on the readout chip (Pixel Unit Cell, PUC). Two PUC columns form a double column, which is independent read at the periphery. Each PUC can be separated in analog and digital part. In the analog, the small signal left by the particle is amplified and sharped, and if it is greater than the local threshold the periphery is noticed, which register the time stamp (bunch cross number). In the digital part, the periphery sends a token through the double column, bypasing the empty pixels. The hit with pixel adress and the time stamp are stored in a data buffer at the periphery waiting for the first level trigger (1LT). In the digital version of the ROC, the size of the data buffer is doubled and the readout speed is increased from 40 to 160 MHz. Prototypes modules with the new ROC need to be tested.

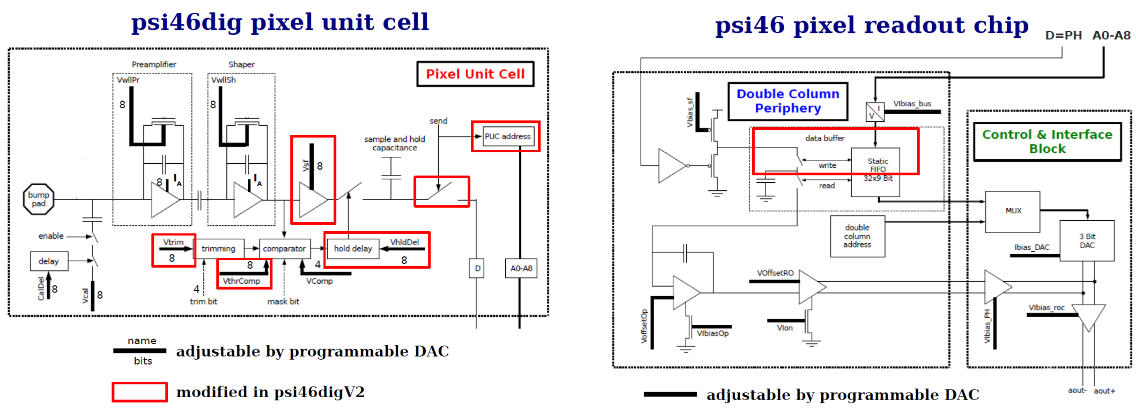

(c) Analog Part of psi46digV2 chip (d) Digital Part of psi46digV2 chip

Figure 2: Read Out Chip

2 Simulation

This project had two principal stages. The Data and the Simulation, the second one it's described in this section. The simultion had two stages as well:Pixelav and Geant4. Those two tools of simulation helped to compare the data of the TestBeam and the simulation.The task was to simulate a position beam passing through a silicon detector with the aim to look at cluster charge deposited.

2.1 Pixelav

Pixelav is a detailed simulation tool of CMS pixel sensors. It includes the following elements [4]:

- A physical model of the charge deposition by primary tracks
- A realistic eletric field map resulting of the resulting of the simultaneous solution of the Poisson's Equation
- Charge carrier transport including mobilities
- Hall Effect and 3D diffusion
- Simulation of radiation damage and charge trapping effects including charge induction
- Electronic noise, response and threshold effects

This simulation have two main steps: electrostatic and electrodynamics. The electrostatic consists in calculating the Electric Field Map of the sensor, based on the design of the pixel sensor and the doping profile. This step is done by the commercial ISE TCAD [5] software. The Electric Field is calculated at the electrodynamic step. The pixelav program has this map as an input and propagates a pion track through a slab of silicon; during the passage e^- and h are created and stored. The pixelav can simulate irradiated and unirradiated sensors; in this project only unirradiated sensors were studied.

Charge deposition in the sensor is modelled using the $\pi - e^-$ elastic cross section from Bichsel [2]. Secondary electrons are created with kinetic energy according to the differential cross sesction, including atomic binding effects. The secondaries loose energy by ionization until the range out or leave the sensor. The range of secondaries is taken from a parameterization. Then the charge transport is the process where the e^- drift to the n side and the holes drift to the n^+ in the presence of the sensor electric field (internal) and the CMS Magnet field (external). This is done by solving numerically the equation of motion for the carries:

$$\frac{d\vec{r}}{dt} = \frac{\mu(q\vec{E} + \mu r_H \vec{E} \times \vec{B} + q\mu^2 r_H^2 (\vec{E} \cdot \vec{B})\vec{B})}{1 + \mu^2 r_H^2 |\vec{B}|^2} \tag{1}$$

where μ is the mobility and r_H is the Hall factor.
The Pixelav output it's a pixel matrix with the numbers of electrons collected in each pixel and this is important to reconstruct cluster and calculate all charge of one cluster. CMS and pixelav uses diferent coordinates systems, so to compare the Data and the simulation, the plots are against the path lenght.

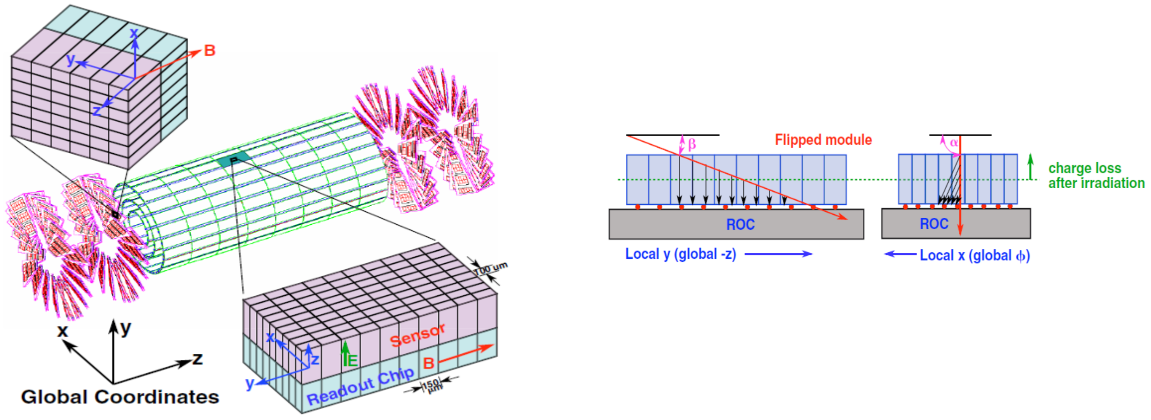

Figure 3: Pixel and Global coordinates

To get the path lenght with α and β,according to the Figure 3: the following formula it's used :

$$l = d\sqrt{1 + \tan^2\alpha + \tan^2\beta} \tag{2}$$

where d = $285\mu m$
This grid is read by the routine *evrd.C* that put a noise (18ke) and creates several histograms, but for the turnscan a cluster charge histogram is interesting to see. The typical plot of the energy deposited it's a Landau distribution shown in Figure 4

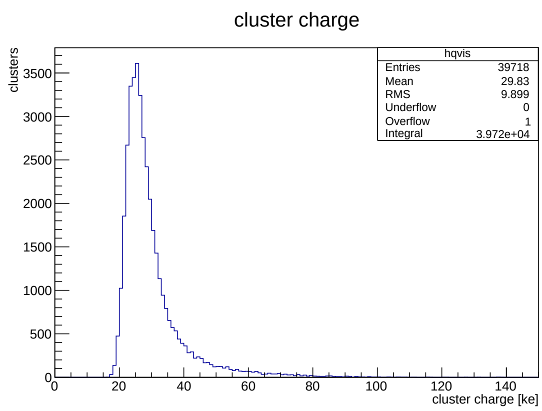

Figure 4: Cluster Charge, 150ke threshold, $\alpha = 22.8$,$\beta = 17.5$

To fit this histogram, there are some model that are going to be introduced in the next section.

2.2 Geant4

Geant4 is a toolkit for the simulation of passage of particle through the matter. In this summer students project, Geant4 was used to simulate the CMS Pixel Sensor. For that was simulated a layer of $285\mu m$ of Silicon with angle of incidence α, so the path lenght of the particle in the sensor it's $285\mu m/cos(\alpha)$ and a beam of 4.4 GeV of e^+. The simulation was based on the Geant4 example `/examples/extended/electromagnetic/TestEm1`. As a result, the spectrum of energy deposited in the silicon layer, shown in Figure 5

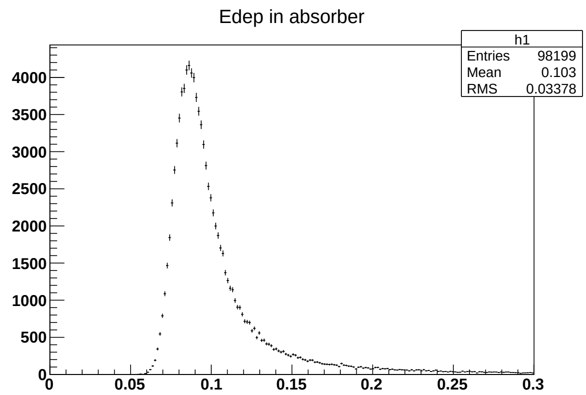

Figure 5: Energy deposited in Silicon [MeV],path length = $300\mu m$

And then, the comparision betwen pixelav and Geant4

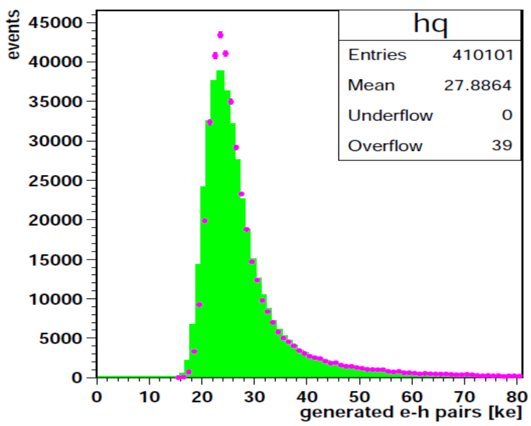

(a) pixelav x Geant4

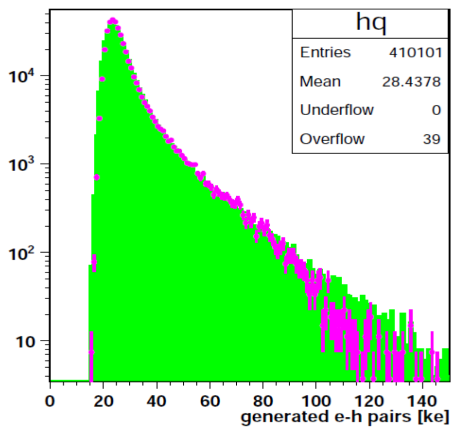

(b) pixelav x Geant4 Log Scale

Figure 6: Pixelav x Geant4

3 Energy Loss Models - Straggling functions

In this section it's introduced the models used to fit the spectrum of energy deposited,there are four of them and the parametes of the best of them were used to compare simulation with data. For this model it's usefull use[6]:
Mean Energy Loss in a single collison

$$\xi = (K/2)\langle Z/A\rangle \left(\frac{x}{\beta^2}\right) \tag{3}$$

where $K/A = 0.307075 MeV g^{-1} cm^2$
for $A = 1 g mol^{-1}$

and x is the thickness in $g cm^{-2}$

So, $x = \rho\delta s$ where δs is the sensor thickness in cm

Maximum Energy Loss in a single collision[1]

$$\varepsilon_{max} = \frac{2m_e c^2 \beta^2 \gamma 2}{1+2\gamma m_e/M+(m_e/M)^2}$$

3.1 Landau Model

In 1944 [3], Landau introduced the straggling function $f_L(\varepsilon, \delta s)$ which gives the probability of a particle passing through an absorver of thickness δs deposited the energy ε small compared with the initial energy.
Here, it's usefull to define the Landau λ:

$$\lambda_L = \frac{\varepsilon-\bar{\varepsilon}}{\xi} - (1-\gamma) - \beta^2 - \ln\frac{\xi}{\varepsilon_{max}}$$

Solving the transport equation, using the Rutherford cross section and neglecting the mean energy loss compare to the maximum energy loss in a single collison,the straggling function is given by:
ε

$$f_L(\varepsilon, \delta s) = \frac{\phi(\lambda_L)}{\xi} \tag{4}$$

$$\phi(\lambda) = \frac{1}{2\pi i}\int_{c+i\infty}^{c-i\infty} \exp\left(u\ln u + \lambda_L u\right) du \quad c \geq 0 \tag{5}$$

$$\gamma = 0.577215\ (Eulers\ constant)$$

$$\varepsilon = actual\ energy\ loss$$

$$\bar{\varepsilon} = average\ energy\ loss$$

So, this model has 3 parameters: $\xi, \bar{\varepsilon}$ and the normalization factor. In ROOT, instead of using the Landau parameters,. it uses the Most Probable Value (Landau Peak) and the Area of the Pdf.Because with there parameteres it's easy to characterize the distribution. The relation between them it's going to be described at section 6. In the Figure 7

3.2 Landau $\otimes$ Gaussian Model

The Landau is convoluted with a Gaussian to simulate noise and non-uniformities of pixels that are in the Data and also simulated by the pixelav.

$$f(\varepsilon, \delta s) = \frac{1}{\sqrt{2\pi}\sigma} \int_{-\infty}^{+\infty} \exp\left(-\frac{(\varepsilon - \varepsilon^{'})^2}{2\sigma^2} \right) f_L(\varepsilon^{'}, \delta s) d\varepsilon^{'} \tag{6}$$

The Gaussian introduces one more parameter, the smearing σ. Shown in Figure 7

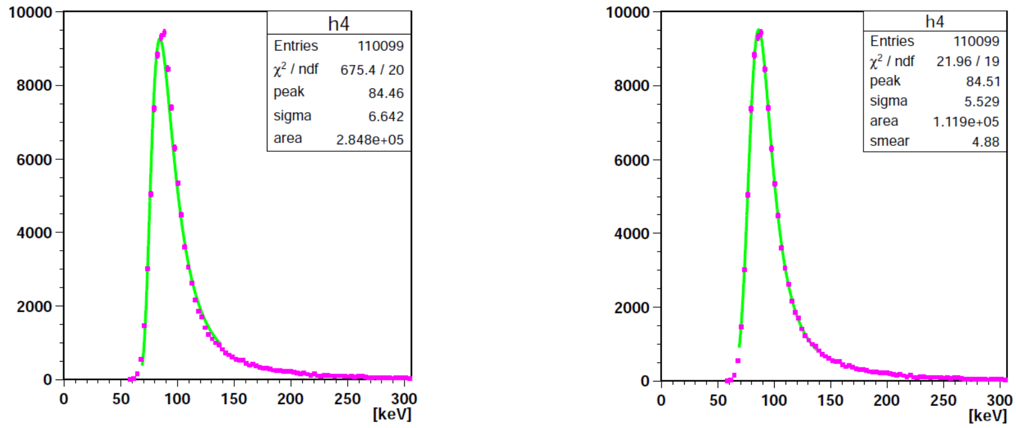

(a) Landau Fit

(b) Landau $\otimes$ Gaussian Fit

Figure 7: Landau Models to Geant4

3.3 Vavilov Model

The Vavilov-Landau theory doesn't assume that the mean energy loss is small compared to the maximum energy loss. It integrates the Rutherford cross section up to the kinematic limit[6].

$$\omega(\varepsilon) = \begin{cases} \frac{\xi}{\varepsilon^2 \delta s}(1 - \frac{\varepsilon\beta^2}{\varepsilon_{max}}) & \varepsilon \leq \varepsilon_{max} \\ 0 & \varepsilon \geq \varepsilon_{max} \end{cases}$$

It introduces a new parameter kappa in the function:

$$\kappa = \frac{\xi}{\varepsilon_{max}} \tag{7}$$

One important issue of this kappa parameter is the limits:

$$\kappa < 0.01 \rightarrow Landau Distribution$$

$$0.01 < \kappa < 10 \rightarrow Vavilov Distribution$$

$$\kappa > 10 \rightarrow Gaussian Distribution$$

After solving the transport equation with the modified cross section and with the kinematic energy limit, the Vavilov Straggling Function as function of Landau's parameter is given by:

$$f_\nu(\lambda_\nu, \kappa, \beta^2) = \frac{1}{2\pi i}\int_{c+i\infty}^{c-i\infty} \phi(s)\ \exp \lambda s\ \ ds \quad c \geq 0 \tag{8}$$

$$\phi(s) = \exp \kappa(1 + \beta^2\gamma)\ \exp \psi(s) \tag{9}$$

$$\psi(s) = s \ln \kappa + (s + \beta^2\kappa) \cdot \left(\int_0^1 \frac{1 - e^{\frac{-st}{\kappa}}}{t}\, dt - \gamma \right) - \kappa\, e^{\frac{-s}{\kappa}} \tag{10}$$

This model has 4 parameters : $\xi, \bar{\varepsilon}, \kappa$ and the normalization factor
Here,as in the Landau model, the parameter are the Vavilov Peak (Most Probable Value), width, κ and the Area. The Fit can be seen in the Figure 8

3.4 Vavilov $\otimes$ Gaussian Model

$$f(\varepsilon, \delta s) = \frac{1}{\sqrt{2\pi}\sigma}\int_{-\infty}^{+\infty} \exp\left(-\frac{(\varepsilon - \varepsilon')^2}{2\sigma^2}\right) f_V(\varepsilon', \delta s) d\varepsilon' \tag{11}$$

The Vavilov model has 4 parameters, with the gaussian σ smearing this model has 5 parameters. It's clear to see that the best fit so far is the Vavilov $\otimes$ Gaussian, so from now on this will be the model used to study the behaviour of the parameters.In the Figure 8

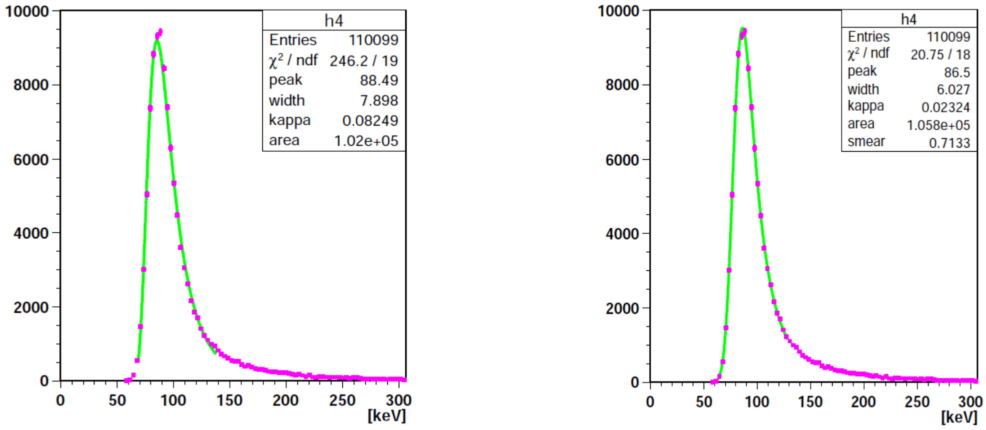

(a) Vavilov Fit

(b) Vavilov $\otimes$ Gaussian Fit

Figure 8: Vavilov Models to Geant4

4 NLOpt

Usually the fits are done MINUIT, but it not gives a good response for this function. So for a good fit, the minimization procedure was done by Non-Linear Optimization [8], that is a open/source library of many non-linear optimization algorithms. The one used in this work was the BOBYQA, that performs a derivative-free bound-constrained optimization using an iteratively constructed quadratic approximation for the objective function. These one was the fastest algorithm and gives a good fit.

5 TestBeam

The DESY II TestBeam facilty takes place at DESY. DESY accelerates positrons and eletrons up to 6.3 GeV, these particles collides with a carbon fiber, generating bremsstralung foton that collides with copper generating eletron-positrons. After that, they pass through a magnet that selects the energy of the particle. At this point the energy can be up to 5 GeV . But it is selected 4.4 GeV because the frequency of particles are greater (700 GHz) In the DESY TestBeam, took at August of 2013, data with different turn and tilt angles was taken to see the response of the sensor. So it can be seen the distribution of the parameters of the fit models. In the next table it shown the runs number, turn, tilt and path length. Angles with this precision comes from the 6 planes of the MIMOSA telescope that has a intrisic resolution of 3.5 μm.

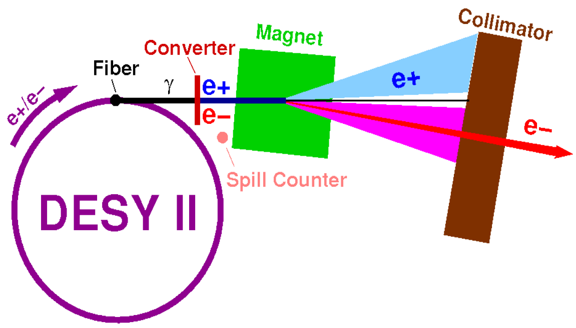

Figure 9: DESY TestBeam

Table 3: Test Beam

Run Number	Turn	Tilt	Path Length [μm]
6208	26.7	18.5	336.3
6214	18.9	16.6	314.4
6259	46.6	21.2	445.0
6292	33.9	19.0	363.1
6320	10.3	20.4	309.0

6 Comparision

In this section it shown the comparision of the collected cluster charge between the simulation and the TestBeam Data. Here, the Data is in blue, pixelav in green and Geant4 in magenta.

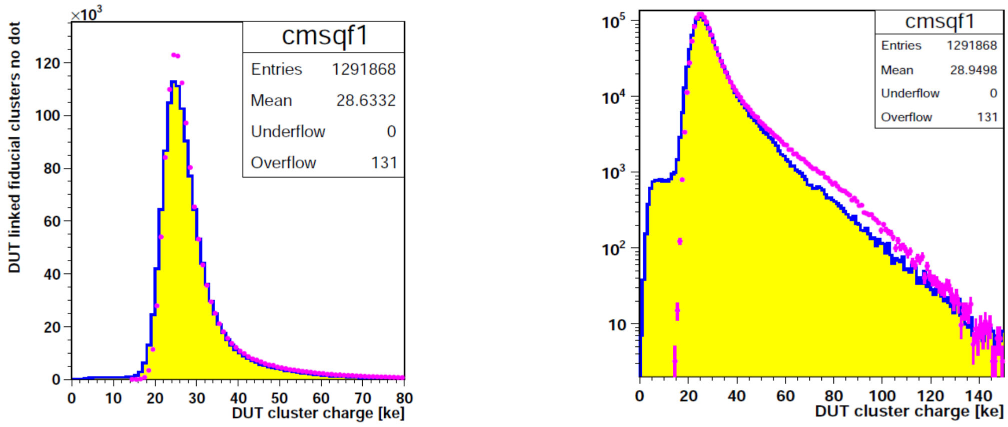

(a) Cluster Charge

(b) Cluster Charge: Log Scale

Figure 10: Collected Cluster Charge: Geant4 x Data

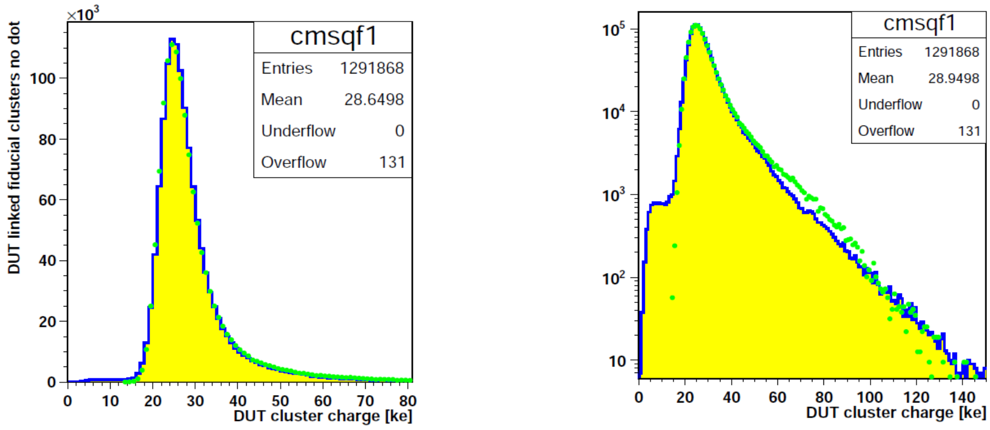

(a) Cluster Charge

(b) Cluster Charge: Log Scale

Figure 11: Collected Cluster Charge: Pixelav x Data

By those plots it is clear to see that the pixelav gives a better explanation for the data, mainly for the tail of the Landau distribution (the δ electrons). The Geant4 gives a higher count fot the peak and overestimates the tail.

7 Parameter Distribution

The Parameter distribution for the Vavilov show how the distribution behaves for different angles, ie different path lenght. The Peak and the Width are shown in Figure 12 and Kappa and Smearing Figure 13, where the are shown the pixelav simulation (green) and the TestBeam Data (blue)

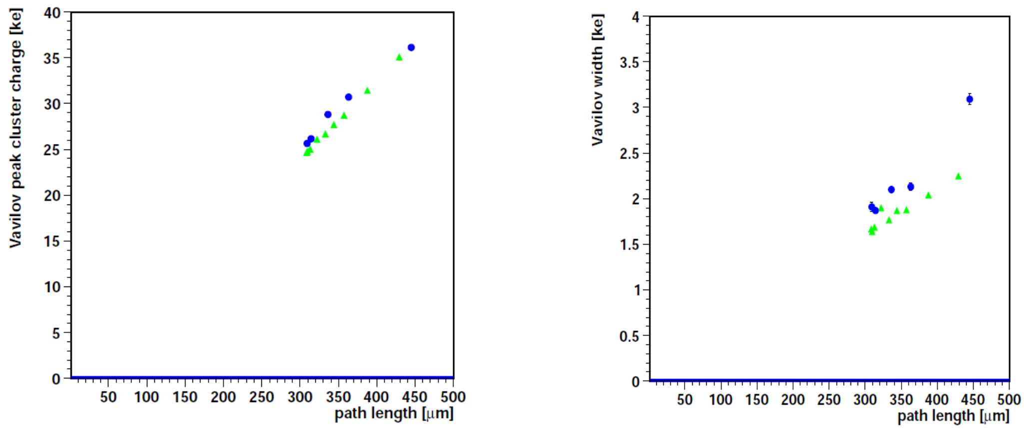

(a) Peak Position (b) Width

Figure 12: Peak and Width distribution

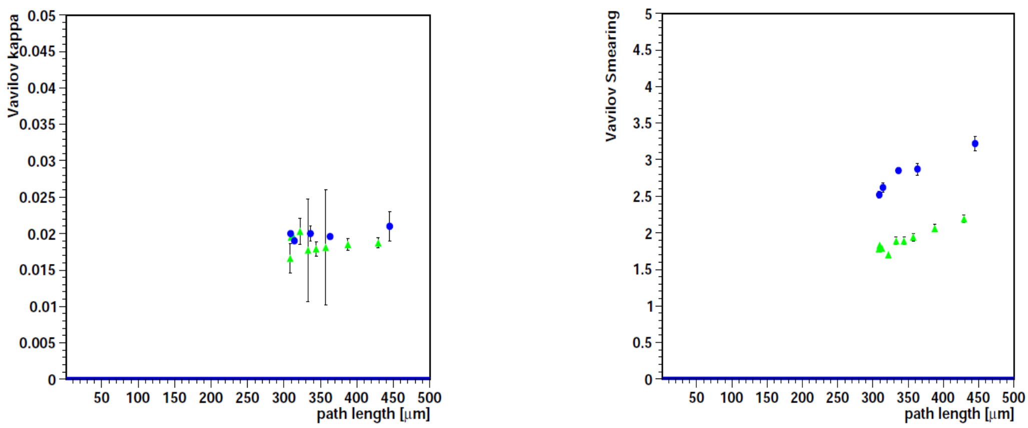

(a) Kappa (b) Smearing

Figure 13: Kappa and Smearing distribution

The Peak and the width have the linear correlation with the path length, as expected. The fact of the Kappa (shape parameter) being almost constant for different paths show that the shape of the distribution remains constant. And for the smearing is expected that grows with the path lenght because more path more noise and also is expected that

the data is greater than the simulation because the noise is greater in the data than in the simulation.
For this comparison, the the peak need to be related, and that it's done by [1]:

$$VavilovPeak = \xi[\ln\frac{2mc^2\beta^2\gamma^2}{I} + \ln\frac{\xi}{I} + j - \beta^2 - \delta(\beta\gamma)] \tag{12}$$

$$VavilovPeak \xrightarrow[\gamma\beta>100]{} \xi[\ln\frac{2mc^2\xi}{(\hbar\omega_p)^2} + j] \tag{13}$$

And the Vavilov width:

$$w = 4\xi \tag{14}$$

where,

$$\xi = (K/2)\langle Z/A\rangle\left(\frac{x}{\beta^2}\right) \qquad x = \rho\delta s$$

Taking in account that the sensor it's silicon ($\rho = 2.33\, g\, cm^{-3}$, Z=14, A=28.08), the velocity of the positron beam is almost c ($\beta = 1$), K is given in equation 3 and the thickness is the path length of the particle

$$w = A \times \delta s[MeV] \tag{15}$$

Using this assumptions, the theoretical value of A is:

$$A = 17.8234 \ \ [eV/\mu m] \tag{16}$$

And we also have the simulation and experimental value of A (the slope of the fit) , by fitting the width of Figure 12

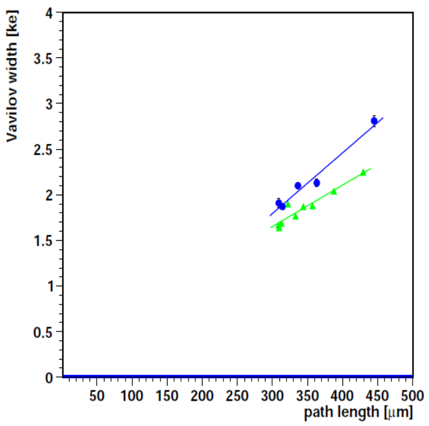

(a) Fit from 300μm to 500μm

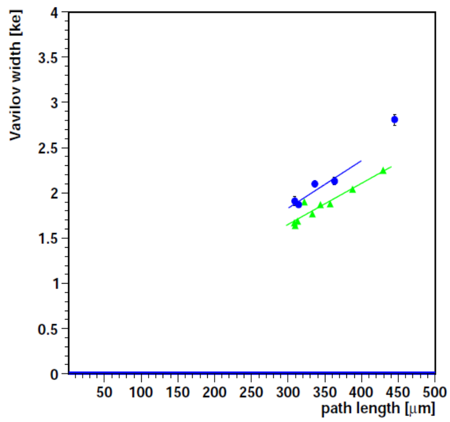

(b) Fit from 300μm to 400μm

Figure 14: Width Fitting

Table 4: Fit from 300μm to 500μm

	Slope $[e/\mu m]$	Error
Data	24.5	1.73
Simlution	16.7	0.77

Table 5: Fit from 300μm to 400μm

	Slope $[e/\mu m]$	Error
Data	19.32	3.42
Simlution	16.7	0.77

In the Figure 14(a) it is possible to see that the simulation gives a result according to the theory, but the Data doesn't. It is clear that the last point is problematic, so trying the fit without it (Figure 14(b)) is clear to see that the last point it is problematic and the Data, Simulation and the Theory Slopes are consistent.

8 Conclusion

The Data and the simulation seems to agree in various points. Pixelav gives good results for the TestBeam but still need some fine tunning to get better results.The Vavilov distruibution seems to explain very good the data and the simulation and can be a usefull tool for studies of δ rays. Also, the parameter distribution plots gives a good notion about the quality of the data, quality of the Fit and how the energy deposition behaviour at different condition. These two tools (pixelav and vavilov distribution) was the main task of these program and seems to worked very well. But, of course, need more tunning and more development.

References

[1] J. Beringer et al. (Particle Data Group), Phys. Rev. D86, 010001 (2012)

[2] H. Bichsel, Rev. Mod. Phys. 60, 663 (1988).

[3] Comparison of calculational methods for straggling in thin absorbers. Hans Bichsel and Roberta P. Saxon, Phys. Rev A 11, 1286 (1975)

[4] Alagz, E. Simulation and beam test measurements of the CMS pixel detector. 2009, University of Zurich, Faculty of Science.

[5] ISE-TCAD, Integrated System Engineering AG, Z rich, Switzerland

[6] New Algorithms for the Vavilov Distribution Calculation and the Corresponding Energy Loss Sampling O. Chibani, IEEE TRANSACTIONS ON NUCLEAR SCIENCE, VOL. 45, NO. 5, OCTOBER 1998

[7] CMS, tracker technical design report CERN-LHCC-98-06.

[8] http://ab-initio.mit.edu/wiki/index.php/NLopt